Lethal and sublethal effects towards zebrafish larvae of microcystins and other cyanopeptides produced by cyanobacteria

Torres, Mariana de Almeida; Jones, Martin R.; vom Berg, Colette; Pinto, Ernani; Janssen, Elisabeth M.-L

DOI:
10.1016/j.aquatox.2023.106689

Document Version
Publisher's PDF, also known as Version of record

Citation for published version (Harvard):
Torres, MDA, Jones, MR, vom Berg, C, Pinto, E & Janssen, EM-L 2023, 'Lethal and sublethal effects towards zebrafish larvae of microcystins and other cyanopeptides produced by cyanobacteria', *Aquatic Toxicology*, vol. 263, 106689. https://doi.org/10.1016/j.aquatox.2023.106689

Aquatic Toxicology 263 (2023) 106689

Contents lists available at ScienceDirect

Aquatic Toxicology

journal homepage: www.elsevier.com/locate/aqtox

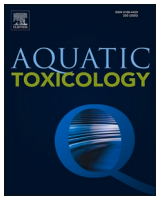

Lethal and sublethal effects towards zebrafish larvae of microcystins and other cyanopeptides produced by cyanobacteria

Mariana de Almeida Torres [a], Martin R. Jones [b], Colette vom Berg [c], Ernani Pinto [d], Elisabeth M.-L. Janssen [c,*]

[a] School of Pharmaceutical Sciences, University of São Paulo, 05508-900, São Paulo, Brazil
[b] School of Biosciences, University of Birmingham, Edgbaston, Birmingham, United Kingdom, B15 2TT
[c] Swiss Federal Institute of Aquatic Science and Technology (Eawag), 8600 Dübendorf, Switzerland
[d] Centre for Nuclear Energy in Agriculture, University of São Paulo, 13418-260, Piracicaba, Brazil

ARTICLE INFO

Keywords:
Cyanobacterial metabolites
Fish toxicity
Cardiotoxicity
Locomotor behaviour
Cyanopeptolin
Microginin

ABSTRACT

Cyanobacterial blooms affect aquatic ecosystems across the globe and one major concern relates to their toxins such as microcystins (MC). Yet, the ecotoxicological risks, particularly non-lethal effects, associated with other co-produced secondary metabolites remain mostly unknown. Here, we assessed survival, morphological alterations, swimming behaviour and cardiovascular functions of zebrafish (*Danio rerio*) upon exposure to cyanobacterial extracts of two Brazilian *Microcystis* strains. We verified that only MIRS-04 produced MCs and identified other co-produced cyanopeptides also for the MC non-producer NPCD-01 by LC-HRMS/MS analysis. Both cyanobacterial extracts, from the MC-producer and non-producer, caused acute toxicity in zebrafish with LC_{50} values of 0.49 and 0.98 $mg_{dw\_biomass}$/mL, respectively. After exposure to MC-producer extract, additional decreased locomotor activity was observed. The cyanopeptolin (micropeptin K139) contributed 52% of the overall mortality and caused oedemas of the pericardial region. Oedemas of the pericardial area and prevented hatching were also observed upon exposure to the fraction with high abundance of a microginin (Nostoginin BN741) in the extract of the MC non-producer. Our results further add to the yet sparse understanding of lethal and sublethal effects caused by cyanobacterial metabolites other than MCs and the need to better understand the underlying mechanisms of the toxicity. We emphasize the importance of considering mixture toxicity of co-produced metabolites in the ecotoxicological risk assessment of cyanobacterial bloom events, given the importance for predicting adverse outcomes in fish and other organisms.

1. Introduction

Cyanobacteria are a diverse group of photosynthetic prokaryotes that, over millions of years of evolution, have adapted to inhabit almost all environments on Earth (Chorus and Welker 2021; Huang and Zimba 2019). In aquatic environments, various cyanobacterial species form blooms, characterised by rapid growth of cyanobacteria into a dense layer of biomass at, or close to, the water's surface. Bloom events have been reported in surface waters across the globe, in particular in regions where there are high nutrient concentrations, high temperatures, longer periods of sunlight, and stratification in lakes (Huisman et al., 2018; Merel et al., 2013). With average regional and global temperatures rising, cyanobacterial bloom events are expected to occur with increasing frequency (Huisman et al., 2018; Merel et al., 2013; Whitton 2017). One main concern associated with high densities of cyanobacteria in aquatic environments is related to their ability to synthesise toxins and a diverse range of bioactive secondary metabolites that include low molecular weight compounds and non-ribosomal oligopeptides, known as cyanopeptides.

From a toxicological perspective, most attention thus far has been paid to one class of cyanopeptide, namely the hepatotoxic microcystins (MCs). This follows from a particularly severe and tragic incident in the city of Caruaru (Brazil, 1996), in which 110 haemodialysis patients developed acute liver failure following exposure to water contaminated with microcystins and cylindrospermopsin, and 60 deaths were attributed to acute intoxication by cyanotoxins from water used for haemodialysis treatment. The World Health Organisation (WHO) responded to this incident by establishing guideline values for exposure through

* Corresponding author.
E-mail address: elisabeth.janssen@eawag.ch (E.M.-L. Janssen).

https://doi.org/10.1016/j.aquatox.2023.106689
Received 3 August 2023; Received in revised form 4 September 2023; Accepted 7 September 2023
Available online 9 September 2023

drinking water for one MC variant, MC-LR (Azevedo et al., 2002; Chorus and Bartram 1999), which was recently extended to include 3 additional cyanobacterial metabolites, namely: anatoxin-a, saxitoxin, and cylindrospermopsin (Chorus and Welker, 2021).

Not only human health but also ecotoxicological risks associated with toxic cyanobacterial blooms have been recognised, with particular focus on aquatic vertebrates in their early life stages. Zebrafish (*Danio rerio*) has emerged as a model species for the assessment of toxicological hazards posed by man-made chemicals, by-products, and naturally occurring biomolecules (Bambino and Chu 2017). During their early life stages, zebrafish are particularly sensitive to chemical-induced toxicity for a number of reasons, including their large surface area, high metabolic rate, absence of mature detoxification pathways, and limited motility, which restricts them to lentic areas where cyanobacteria frequently form scums or lentic populations dominate (Malbrouck and Kestemont 2006; Di Paolo et al. 2015). Exposure of zebrafish embryos to cyanobacterial extracts containing microcystins has been shown to induce lethal effects, with LC_{50} values ranging from 0.032 to 0.67 $mg_{dw\_biomass}$/mL, expressed as mg dry weight of extracted biomass equivalents per mL exposure medium (Blagojevi et al. 2021; Pipal et al., 2020; Malbrouck and Kestemont 2006). Studies exploring the acute toxicity of pure microcystins in zebrafish embryos are limited. Wei et al. (2020) reported recently the first LC_{50} for MC-LR with 2.79 mg/L, expressed as mg MC-LR per litre exposure medium, emphasizing the lethal role of microcystins. However, two recent studies also reported comparable lethal effects on fish larvae upon exposure to cyanobacterial extracts not containing microcystins (LC_{50} varied from 0.3 to 0.4 $mg_{dw\_biomass}$/mL, Pipal et al., 2020; Fernandes et al., 2019). In addition, sublethal effects were observed in zebrafish upon exposure to cyanobacterial extracts, including oedema of the digestive system, curvature of the tail, craniofacial and jaw deformations, also when no microcystins were detectable in the extracts (Jacinavicius et al., 2023; Pipal et al., 2020).

Across cyanobacterial species, 2425 cyanobacterial metabolites have been reported to date. Of these, approximately 65% are classified as cyanopeptides, including 318 microcystins (Jones et al., 2021; Janssen et al., 2023). The latter have received the majority of attention in terms of toxicological research, though evidence exists to suggest other cyanopeptide classes demonstrate toxicologically-relevant bioactivity (Janssen, 2019). Even though much less research has been carried out thus far for cyanopeptides beyond microcystins, enzyme inhibition has most frequently been attributed to be one of their functions. Cyanopeptolins and aeruginosins are active against serine proteases (e.g., thrombin, trypsin, chymotrypsin, plasmine, and factor VII) (Huang and Zimba 2019; Köcher et al., 2020; Mazur-Marzec et al., 2018; Nagarajan et al., 2013). Microginins can inhibit zinc metalloproteases, such as certain aminopeptidases and angiotensin-converting enzyme (ACE, involved in blood pressure regulation) (Ishida et al., 2000; Lodin--Friedman and Carmeli 2018; Paiva et al., 2017). Consequently, it can be hypothesized that there may be a link between (sub)lethal effects observed in zebrafish and the presence of other cyanopeptides co-produced by cyanobacteria. However, despite the reported adverse effects in fish of complex cyanobacterial extracts, it is not yet clear which cyanopeptides drive toxic effects in these mixtures and through which mechanisms they induce adverse health effects.

The aim of this study was to link lethal and sublethal effects in the zebrafish model, *Danio rerio,* to cyanopeptides beyond microcystins using extracts of two Brazilian cyanobacterial strains (*Microcystis* MIRS-04 and NPCD-01), and to decipher the contribution of constituent metabolites to observed phenotypes. We first demonstrated that both strains cause acute toxicity and morphological alterations, despite the NPCD-01 strain not producing microcystins. Using semi-purified fractions of cyanobacterial extracts, we were also able to discover that a cyanopeptolin contributed to more than 50% mortality of the MC-producing MIRS-04 strain. Our work also revealed that exposure to microcystins and other cyanopeptides can cause oedemas of the pericardial region, prevented hatching, and decreased locomotor activity in surviving zebrafish. Overall, the co-production of these other bioactive metabolites with known toxins such as microcystins emphasizes the need to consider multiple stressors during cyanobacterial blooms, and further research on mixture toxicity is recommended.

2. Experimental section

2.1. Materials

Methanol and acetonitrile were purchased from Thermo Scientific™ (Optima®LC/MS 99.9%). Nanopure water was from a NANOpure® 21 water purification system (Barnstead from Thermo Scientific). Formic acid (98–100%) and ethanol (absolute for analysis, EMSURE® ACS ISO Reag. pH Eur) were purchased from Sigma Aldrich. Nodularin and microcystin reference standards with >95% purity (MC-LR, MC-YR, MC-RR, MC-LF, MC-LA, MC-LW, MC-LY, [D-Asp^3]MC-LR, MC-HilR) were acquired from Enzo Life Science (Lausen, Switzerland) and [D-Asp^3,*E*-Dhb^7]MC-RR (also >95% purity) from CyanoBiotech GmbH (Berlin, Germany). Aerucyclamide A was kindly provided as a purified bioreagent in dimethyl sulfoxide by Prof. Karl Gademann (University Zurich, Switzerland). Bioreagents (all >90% purity) for aeruginosin 98B, cyanopeptolin A, cyanopeptolin D, anabaenopeptin A, anabaenopeptin B, and oscillamide Y were obtained from CyanoBiotech GmbH (Berlin, Germany). All salts used for culture medium preparation were analytical grade.

2.2. Cyanobacterial cultures

Cyanobacterial strains *Microcystis panniformis* (MIRS-04, isolated from the Samuel Reservoir in Rondônia, Brazil), and *Microcystis aeruginosa* (NPDC-01, isolated from a sewage treatment plant in Cidade de Deus, Rio de Janeiro, Brazil) were obtained from the culture collection of the Laboratory of Ecophysiology and Toxicology of Cyanobacteria, at the Federal University of Rio de Janeiro (Brazil).

Strains MIRS-04 and NPCD-01 were cultivated in the Laboratory of Toxins and Natural Products of Algae and Cyanobacteria at the University of São Paulo - Brazil, using ASM-1 medium with pH adjusted to 7.5, for 20 days (Gorham et al., 1964) (Table SI1). Culture flasks were maintained under a 12 h light/dark photoperiod, with light intensity of 20 μmol photons m^{-2} s^{-1}, continuous aeration, and temperature of 24 ±2 °C. After 20 days of growth, cells were harvested by centrifugation (9000 rpm at 15 °C, 10 min). The resulting biomass was stored at −20 °C, lyophilized (−55 °C, 500 μHg, 24 h, L101 Liotop® lyophilizer, Liobras, Brazil), and sent to the Swiss Federal Institute of Aquatic Science and Technology (Eawag) for high performance liquid chromatography-high resolution mass spectrometry/tandem mass spectrometry (HPLC-HRMS/MS) analyses, fractionation, and toxicity testing.

2.3. Extraction of lyophilised cyanobacterial biomass and fractionation procedure

Lyophilised cyanobacterial biomass was extracted using a solution consisting of 7:3 v/v methanol:water at a ratio of 1 mL solution per 50 mg dry weight of biomass. This solution was added at room temperature to the biomass at 20 μL $mg_{dry\ weight}^{-1}$ and vortex mixed for 30 s. The resulting slurry was sonicated in an ultrasonic bath (VWR, Ultrasonic cleaner USC-THD, level 6, 15–19 °C) for 10 min to homogenise the sample, followed by centrifugation (Eppendorf Centrifuge 5427 R, 10 min, 10 °C and 4000 rcf) to pellet out debris. Supernatant was transferred to a new glass vial. Pelleted material was re-extracted in the same way, with the resulting supernatant combined with that from the first round of extraction. In total, 1 g each of lyophilised MIRS-04 and NCPD-01 biomass was extracted.

Upon completing extraction, supernatants were placed into a

Turbovap, wherein a gentle stream of nitrogen was applied (>0.8 L/min, 40 °C, TurboVap LV, Biotage) to evaporate excess methanol. Resulting extracts (ca. < 5% methanol) were then diluted with nanopure water, the exact mass recorded (±0.001 g), centrifuged (Eppendorf Centrifuge 5427 R, 10 min, 10 °C, and 4000 rcf), and filtered (PTFE syringe filters, 0.45 μm) into fresh glass vials.

Filtered extracts were fractionated using an UltiMate™ 3000 UHPLC System (Thermo Scientific™) coupled with a FoxyJr® Fraction Collector. Fractionation was performed over a Kinetex® LC column (C18, 5 μm particle size, 100 Å pore size, 150×4.6 mm, Phenomenex®), fitted with in-line filter (BGB®), using a binary gradient of nanopure water (A) and methanol (B) maintained at 30 °C and supplied at 1.2 mL/min, as follows: 0 min, 20% B; 4 min, 50% B; 20 min, 68% B; 21 min, 95% B; 25 min, 95% B; 25.1 min, 20% B; 30 min, 20% B. Filtered extracts were injected at 100 μL. Fractions were collected into 50 mL amber glass vials at 2 min intervals throughout the LC gradient, starting at minute 4 and ending at minute 26, resulting in 11 distinct fractions. The first 4 min of the chromatographic run were diverted to waste to exclude salts and highly polar compounds (beginning) from fractions, whereas the final 4 min were diverted to waste during re-euqilibration of the column. Blank injections of nanopure water were run after every 5th sample, during which fractions were not collected. After every 15th injection, the analytical column was flushed with LC-MS grade acetonitrile and then re-equilibrated for further fractionation runs.

Collected HPLC fractions were evaporated to dryness using a Syncore® Analyst R-12 (BÜCHI Labortechnik AG, shaker temperature 55 °C, lid temperature 60 °C, 175 rpm, final pressure at 20 mbar, cooling system at 4 °C). Dried fractions were resuspended in ethanol overnight (LABWIT ZWYR-D2403 incubator, 100 RPM, 12 °C), followed by gravimetric dilution to 80:20% w/w ethanol:water, prior to storage at −20 °C.

2.4. Analysis of cyanopeptides by LC-HRMS/MS

Concentrated HPLC fractions derived from extracts of both cyanobacterial strains were diluted with nanopure water (99-fold dilution) and analysed by high-performance liquid chromatography (Dionex UltiMate3000 RS pump, Thermo Fisher Scientific) coupled with high-resolution tandem mass spectrometry (HRMS/MS, Orbitrap Fusion Lumos and Exploris 240, Thermo Scientific). Samples were injected into the HPLC system (20 μL) using a CTC Analytics autosampler, and chromatographic separation was achieved over a Kinetex® LC column at 40 °C (C18, 2.6 μm particle size, 100 Å pore size, 100×2.1 mm, Phenomenex®), fitted with C18 guard-cartridge and inline filter (BGB®). Samples were eluted using a binary gradient of nanopure water (solvent A) and methanol (solvent B), both containing 0.1% v/v formic acid (10 to 95% of B in 25 min) supplied at a flow rate of 255 μL/min (Natumi and Janssen, 2020a). HPLC eluates were introduced into the HRMS/MS system (Orbitrap Fusion Lumos or Exploris 240) via an electrospray ionization source (ESI) operated as follows: positive ionization mode with capillary voltage of 3.5 kV, 320 °C capillary temperature, 40 arbitrary units (AU) sheath gas, 10 AU auxiliary gas, and 275 °C vaporizer temperature. Full scan data was acquired between 450 and 1350 m/z at a resolution of 120,000 (full width-half maximum at 200 m/z ($FWHM_{200m/z}$)) and with: automated gain control (AGC) of $5{\cdot}10^4$, maximum ion injection time of 50 ms, 1 microscan, and 40% S-lens RF setting. Data-dependant acquisition of MS/MS (MS^2) scans was guided by an inclusion list, consisting of m/z values for the singly and doubly charged protonated forms of all cyanopeptides present in the publicly available CyanoMetDB database (Version01, Jones et al., 2021). The feature 'pick others' was set when no targets of the inclusion list were detected. For each MS^2 precursor ion, data-dependant MS^2 product ion spectra were independently acquired at normalised collision energies of 15%, 30%, and 45%, using a resolution setting of 15,000 ($FWHM_{200m/z}$), AGC target of $1{\cdot}10^4$, and maximum ion injection time of 22 ms.

2.5. Data processing and cyanopeptide quantification

HPLC-HRMS/MS data were processed using Skyline 20.1 (MacCoss Lab Software). Structural annotations were assigned through comparison to the CyanoMetDB database, as well as 18 standards or bioreagents analysed alongside HPLC fractions (these being used to generate external calibration curves). In assigning annotations, we followed the identification scheme and levels (Level 1–5) previously described for micropollutants (Schymanski et al., 2014), and adapted for cyanopeptides (Filatova et al., 2021; Natumi et al., 2021, and Janssen 2021; Natumi and Janssen 2020b). Tentative candidates (level 3) were annotated by screening MS^1 data with CyanoMetDB, following the criteria: exact mass error <3.0 ppm; isotopic pattern fit of >0.93, considering the precursor and at least two isotopes, and based on Skyline idotp score; and consistent retention time (RT) across samples. These allowed to link the proposed molecular formula to compounds in CyanoMetDB considering but not differentiating between isomers. Probable structures were annotated (level 2) based on diagnostic evidence from the fragmentation data (2b) and through spectral library matching (2a). Structural identification (level 1) was achieved where these criteria matched one of our reference standards or bioreagents. For most suspects, no analytical standards are commercially available, nor are reference spectra deposited in open-source databases (e.g., MassBank Europe). For those candidates tentatively annotated through suspect screening, we manually evaluated MS^2 spectra with support from *in silico* molecular fragmentation data generated from CyanoMetDB using MetFrag (Ruttkies et al., 2016). We also considered previously published MS^2 spectra from the primary references listed in CyanoMetDB to increase the confidence of identification and differentiate between structural isomers.

The most abundant peptides were quantified by external calibration with the corresponding standard or bioreagent, when possible. For those cyanopeptides for which no reference standard or bioreagent were available, quantification was based on external calibration against the MC-LR regression model ("calibration curve"), yielding MC-LR equivalent concentrations. We acknowledge that differences may exist between MC-LR and the other cyanopeptides quantified in terms of their response factors and any associated matrix effects. This is a commonly applied approach (Filatova et al., 2021; Natumi et al., 2021; Natumi et al., 2020a), and despite potential limitations and quantitative errors that can be introduced, we adopted it to aid comparison with other studies. Concentrations were only reported when the peak area was above the limit of quantification (LOQs) of the respective regression model.

For the most apolar HPLC fractions (fraction #9, 22 to 24 min; and fraction #10, 24 to 26 min) molecular networks were generated using the Global Natural Products Social Molecular Network (GNPS) platform (available at http://gnps.ucsd.edu, UC San Diego, La Jolla, CA, USA). The raw MS data were converted into mzXML file format and uploaded to GNPS. GNPS molecular networking parameters were set as follows: precursor ion mass tolerance, 0.02 Da; fragment ion mass tolerance, 0.02 Da; min pairs cos, 0.7; network topk, 10; minimum matched fragment ions, 6; minimum cluster size: 2. Additional filters included: precursor window, peaks in a 50 Da window, and spectra from G6 as blanks before networking. Spectra were automatically searched for annotation against the GNPS spectral libraries (thresholds fixed for cosine score >0.7 and at least six matched peaks). The molecular network outputs were enhanced with the MolNetEnhancer tool to provide a more comprehensive chemical overview of the metabolites matched in the given fractions (Ernst et al., 2019). Molecular networks were visualized using Cytoscape 3.8.2.

2.6. Preparation of the HPLC fractions for toxicity tests

Each HPLC fraction (in 80:20% w/w ethanol:water solution) was prepared for use in toxicity tests by transferring a defined aliquot into an independent Büchi Syncore® Analyst R-12 evaporator vial with 1 mL appendix. Therein, the fraction aliquot underwent vacuum-assisted

evaporation to displace ethanol, leaving sample constituents behind in water (shaker temperature 55 °C, lid temperature 60 °C, 175 rpm, 20 mbar, cooling system at 4 °C). Upon completion, residual liquid in the evaporator vial was transferred to a pre-weighed, glass storage vial. The evaporator vial was then rinsed twice with nanopure water, with each rinse being transferred to the storage vial. Thereafter, the contents of the storage vial were gravimetrically adjusted to a defined mass using nanopure water, followed by dilution 1:1 (v/v) with aerated, double-concentrated Zebrafish culturing medium. Solvent controls were prepared in the same way, using 80:20% w/w ethanol:water solution as input.

Note, for testing the toxicity of the "whole extract" (minus any components removed during fractionation), the same process was applied, albeit with a fixed volume/mass of each HPLC fraction being added to the evaporator vial prior to drying. The resulting sample is herein referred to as the *pool* or *pooled fractions*.

The following steps consisted of preparing the exposure solution's dilution series with aerated culture medium. The concentrations of the pooled and isolated fractions were calculated to reflect portion of the biomass extracted that resulted in each fraction as the ratio of the mg dry weight biomass to the mL exposure solution. For the toxicity tests, the concentration was calculated considering the initial concentration of the pool or individual fractions, the mass of the aliquot taken, and the final volume of the exposure solution in culture medium.

2.7. Zebrafish maintenance and embryo-larval experiment procedures

Zebrafish, *Danio rerio*, (strain WM, mixed wildtype) were maintained in the fish facility of Eawag, under standard and controlled conditions, and in accordance with relevant Swiss animal protection law. To ensure that variability was being introduced and evaluated in the experiments, fertilized eggs were collected and selected from approximately 200 adult fish, which were maintained in 12 L tanks at a density of one fish per litre, at 26 ± 1 °C and under a photoperiod of 14/10 h light/dark. Tanks were connected to a recirculating flow-through system supplied with a mixture of tap and desalted water (1:1). Fish were fed twice a day on weekdays, and once a day over weekends, with granulate (ZebraFeed, Sparos, Portugal) and live food (*Artemia salina* nauplii). For breeding, spawning trays were added to the tanks by the end of the day, with eggs collected the following morning, approximately 1 h post-fertilization. The eggs were rinsed and kept in aerated culture medium (294.0 mg/L $CaCl_2{\cdot}2H_2O$, 123.2 mg/L $MgSO_4$ $7H_2O$, 64.7 mg/L $NaHCO_3$, and 5.7 mg/L KCl in nanopure water, according to ISO-7346/3 guideline) (ISO 1996). The collected eggs were then pre-exposed in Petri dishes (4 mL of pre-exposure solution) and sorted to ensure only fertilised eggs were transferred to the exposure plate (48-well plates, Greiner Bio-One, Austria). The final volume in each well was 500 μL. Exposure plates were covered with adhesive foil throughout the exposure period, and kept in the incubator at the same conditions mentioned above. Up to 5 different concentrations were tested for the pooled and individual fractions. Relevant controls were performed in all tests, namely 4 mg/L 3,4-dichloroaniline (positive control, as suggested by the OECD test guideline number 236/2013), aerated culture medium (negative controls), and solvent control (from sample preparation, as explained above). A total of 21 fertilised embryos were used per exposure concentration, 32 embryos for the solvent and negative controls, and 16 embryos for the positive control. As specified in OECD test guideline (OECD 2013), each embryo was treated as an independent replicate for statistical analysis.

Daily observations of lethal and sublethal effects were performed following OECD test guideline 236 for Fish Embryo Acute Toxicity (FET) tests (OECD 2013) and Kimmel et al. (Kimmel et al., 1995), using a Leica S8APO stereo microscope. The exposure lasted 120 h, and on the final day, in addition to the lethal and sublethal endpoints, morphological, cardiological, and behaviour measurements were recorded, as detailed below. The pH, dissolved oxygen, and temperature were also measured in both the control media and the highest concentration exposure medium, on both the first and last day of the FET test. All experiments were carried out according to relevant animal protection guidelines.

2.8. Heart rate and morphological measurements of zebrafish larvae

Heart rate and morphological measures of exposed fish and associated controls were performed on the final day of the experiment (day 5, 120 h). Larvae were anaesthetized with 160 mg/L of ethyl 3-aminobenzoate methanesulfonate (MS222; Sigma-Aldrich), a level of anaesthesia shown to not influence zebrafish heart rates and applied in previous work (Fitzgerald et al., 2019).

A 15-second video was recorded at 30 frames per second for each larvae orientated in the lateral position (Media Recorder 4 software, version 4.0; Noldus, Netherlands), using a Basler acA2000–165 μM camera installed on a Leica S8APO stereo microscope.

The acquired videos were processed using DanioScope Software (version 1.2.206; Noldus, Netherlands), wherein heart rate and morphology parameters were measured. The heart area was manually defined in each video, with the software calculating the number of beats per minute using a power plot spectrum of the frequencies extracted from an activity signal. Body length (from nose to tip of the tail; mm), eye size, and swim bladder area (both from the lateral view of the larvae; mm^2) were also measured manually, using one picture frame from the video. The same calibration profile was used to analyse all images to minimise bias during image processing.

2.9. Behaviour tracking and data analysis

To assess whether behavioural responses were affected in exposed larvae, behaviour was recorded at 120 hpf using the DanioVision Observation Chamber (v. DVOC-0040T; Noldus, Netherlands), consisting of a Gigabit Ethernet video camera fitted with infrared and white-light sources and a transparent multi-well plate holder. A standard PC system with the EthoVision XT13 software (version 13.0.1220, Noldus, Netherlands) connected to the camera recorded the videos for later analysis of locomotor activity. All behaviour experiments were conducted in a temperature-controlled room maintained at 26 ± 1℃.

The behaviour assay, frequently referred to as light-dark transition test, consisted of different phases: acclimation period of 20 min in light, to allow the fish to adjust (settle baseline movement) (I); 20 min of spontaneous swimming behaviour in light (hereafter referred to as "spontaneous") (II); two alternated dark intervals of 10 min (III and V); and two alternated light intervals of 10 min (IV and VI).

Using the EthoVision XT13 software, fish were re-tracked in the recorded videos using a non-live tracking mode, allowing a static subtraction of the background and reducing tracking artefacts. Distance moved was chosen as parameter to cross-compare experimental groups.

2.10. Statistical analysis

A non-linear regression model (Prism 9.4.1, GraphPad Software, Inc., San Diego, California) was used to estimate the concentration at which HPLC fractions, derived from *M. aeruginosa* (NPCD-01) and *M. panniformis* (MIRS-04), induced mortality in 50% of exposed zebrafish larvae (LC_{50}). From this regression model, the slope factor (HillSlope) and goodness of fit (R^2) were assessed. Other statistical analyses (such as Kolmogorov–Smirnov's normality test, Kruskal–Wallis H test, post-hoc Dunn's for multiple comparisons), were also performed using Prism 9.4.1. The significance level considered was $p < 0.05$.

3. Results and discussion

HPLC-based fractionation was used to semi-purify crude extracts of two *Microcystis* strains originally isolated from Brazilian waters (do Nascimento et al. 2021; Silva-Stenico et al. 2011), namely: *Microcystis*

panniformis strain MIRS-04, a microcystin producer, and *Microcystis aeruginosa* strain NPCD-01, a non-producer of microcystins. Resulting HPLC fractions were analysed by HPLC-HRMS/MS to assess their cyanopeptide composition, while zebrafish embryo toxicity tests were conducted to assess associated toxicological effects.

3.1. Cyanopeptides produced by the two Microcystis strains

For each HPLC fraction analysed by HPLC-HRMS/MS, cyanopeptide structures were assigned based on suspect screening of full scan data against CyanoMetDB (version 1, 2021) and MS^2 spectral annotations (Figures SI15-SI26). These analyses revealed several microcystin and cyanopeptolin variants in HPLC fractions derived from MIRS-04 (Table 1, Fig. 1). In terms of total peak area, the four most abundant cyanopeptides in MIRS-04 were micropeptin K139 (MP K139, 74.9%), microcystin-LR (MC-LR, 11.9%), cyanopeptolin 972 (CP 972, 6.3%) and cyanopeptolin 958 (CP 958, 3.7%), with [D-Asp^3]MC-LR, [D-Asp^3, $ADMAdda^5$]MC-LHar and cyanopeptolin 1014 (CP 1014) being minor components. As for HPLC fractions derived from NPCD-01, the most abundant compounds based on peak area were nostoginin BN741 (NG BN741, 78.4%), microginin FR6 (MG FR6, 9.6%), cyanopeptolin 959 (CP 959, 6.8%), and microginin SD755 (MG SD755, 5.2%). We acknowledge that peak areas do not necessarily accurately reflect the absolute quantities of each compound present across the samples, due to differing ionisation efficiencies of each compound prior to mass spectrometry detection. However, we judge this approach as a useful tool for a first assessment of the abundance of different compounds produced by the strains and their distribution through the HPLC fractions when reference standards are not available commercially. The cyanopeptides identified herein mostly agree with those reported previously by Fernandes et al. (2019), despite differences in the extraction procedure. The only major difference was nostoginin BN741, which in the present study was found to be the major microginin in NPCD-01.

The concentration of MC-LR could be quantified with an authentic reference standard and expressed relative to the quantity of biomass extracted. In the MIRS-04 extract, the MC-LR concentration was found to be 1.13 μg/mg of dry weight biomass in the present study, versus 1.50 μg/mg in the study by Fernandes et al. (2019), and such variation is likely linked to differences in the extraction protocol.

3.2. Acute toxicity towards zebrafish embryos

Zebrafish embryos were exposed to HPLC fractions of extracted MIRS-04 and NPCD-01 biomass, in accordance with OECD test guideline No. 236 (2013). Throughout the exposure, zebrafish were inspected for acute and sublethal effects, with behavioural and morphological effects also assessed at the final exposure time point (120 hpf). *Pooled fractions* for MIRS-04 and NPCD-01, prepared by combining aliquots of all associated HPLC fractions, were initially assessed for acute toxicological effects, before assessing the contribution of individual fractions.

Exposure to *pooled fractions* revealed a dose-dependant relationship between zebrafish mortality at the 120 hpf time point for both cyanobacterial strains (Fig. 2A and Figure SI2). The concentration of *pooled fractions* that induced mortality in 50% of larvae (LC_{50} value), expressed relative to mg of dry weight biomass per mL exposure medium, was 0.49 (0.42–0.58) $mg_{dw\_biomass}$/mL for MIRS-04 and 0.98 (0.89–1.07) $mg_{dw\_biomass}$/mL for NPCD-01 at 120 hpf.

For both strains, mortality occurred by 24 hpf and did not further increase until the final time point at 120 hpf (Figure SI6). The LC_{50} values for MIRS-04 and NCPD-01 *pooled fractions* showed the same trend but were 2-fold and 3-fold higher, respectively, compared to values measured previously using native Brazilian fish larvae *Astyanax altiparanae* (0.24 and 0.32 $mg_{dw\_biomass}$/mL of the aqueous extract, respectively) (Fernandes et al., 2019). The present study further supports earlier observations that *Microcystis* strain NPCD-01 does not produce microcystins nor any other recognized cyanotoxins (i.e., anatoxin-a, cylindrospemopsin, saxitoxin), yet causes significant acute and lethal toxicity in both fish species (Fernandes et al., 2019). To further investigate the contribution of individual cyanopeptides or subsets of cyanopeptides, to the observed mortality in the pooled fractions, zebrafish embryos were exposed to individual HPLC fractions from each strain.

For the MIRS-04 extract, a micropeptin K139-dominated fraction (fraction #7 with RT 16–18 min, 93% by peak area, Figure SI1C) induced dose-dependant mortality, with maximum mortality at 120 hpf of 52% at the two highest exposure concentrations (8.74 and 3.49 $mg_{dw\_biomass}$/mL equivalents, Fig. 2B). By contrast, the two highest concentrations of the MIRS-04 *pooled fractions* (5.43 and 2.17 $mg_{dw\_biomass}$/mL equivalents) induced 100% mortality at 120 hpf.

For reference, the dose-response data based on peak area and MC-LR equivalent concentrations for micropeptin K139 are presented in Figure SI3. Despite 100% mortality having not been reached by 120 hpf, an LC_{50} value at 120 hpf was estimated for the micropeptin K139-dominated fraction to be 6.21 (4.55–8.47) $mg_{dw\_biomass}$/mL, almost 15-fold higher compared to the *pooled fractions* resembling the total extract. Unlike the *pooled fractions*, the micropeptin K139 fraction showed an increase in mortality between 24 and 72 hpf at the two highest exposure concentrations (8.74 and 3.49 $mg_{dw\_biomass}$/mL,

Table 1
Cyanopeptides annotated as tentative candidates based on matching MS1 data against CyanoMetDB (level 3), probable structures based on diagnostic evidence of MS^2 (level 2) or identified as confirmed structures by reference standard (level 1) in methanolic extracts of *Microcystis panniformis* (MIRS-04) and *Microcystis aeruginosa* (NPCD-01).

Microcystis panniformis (MIRS-04)						
Cyanopeptides	class	molecular formula	precursor ion type	precursor m/z	% by peak area	level of confidence
Micropeptin K139	cyanopeptolin	$C_{47}H_{74}N_{10}O_{13}$	[M+H]+	987.5509	74.9	Level 2b
MC-LR	microcystin	$C_{49}H_{74}N_{10}O_{12}$	[M+H]+	995.5560	11.9	Level 1
Cyanopeptolin 972	cyanopeptolin	$C_{46}H_{72}N_{10}O_{13}$	[M+H]+	973.5353	6.3	Level 2b
Cyanopeptolin 958	cyanopeptolin	$C_{45}H_{70}N_{10}O_{13}$	[M+H]+	959.5197	3.7	Level 2b
[D-Asp^3]MC-LR	microcystin	$C_{48}H_{72}N_{10}O_{12}$	[M+H]+	981.5403	1.2	Level 1
Cyanopeptolin 1014	cyanopeptolin	$C_{49}H_{78}N_{10}O_{13}$	[M+H]+	1015.5822	0.7	Level 2b
[D-Asp^3,$ADMAdda^5$]MC-LHar	microcystin	$C_{50}H_{74}N_{10}O_{13}$	[M+H]+	1023.5509	0.7	Level 3
MC-LY	microcystin	$C_{52}H_{71}N_7O_{13}$	[M+H]+	1002.5182	0.3	Level 1
Microcystis aeruginosa (NPCD-01)						
Cyanopeptides	class	molecule formula	precursor ion type	precursor m/z	% by peak area	level of confidence
Nostoginin BN741	microginin	$C_{39}H_{59}N_5O_9$	[M+H]+	742.4385	78.4	Level 2b
Microginin FR6	microginin	$C_{39}H_{57}N_5O_9$	[M+H]+	740.4229	9.6	Level 3
Cyanopeptolin 959	cyanopeptolin	$C_{43}H_{61}N_9O_{14}S$	[M+H]+	960.4131	6.8	Level 2b
Microginin SD755	microginin	$C_{40}H_{61}N_5O_9$	[M+H]+	756.4542	5.2	Level 2b

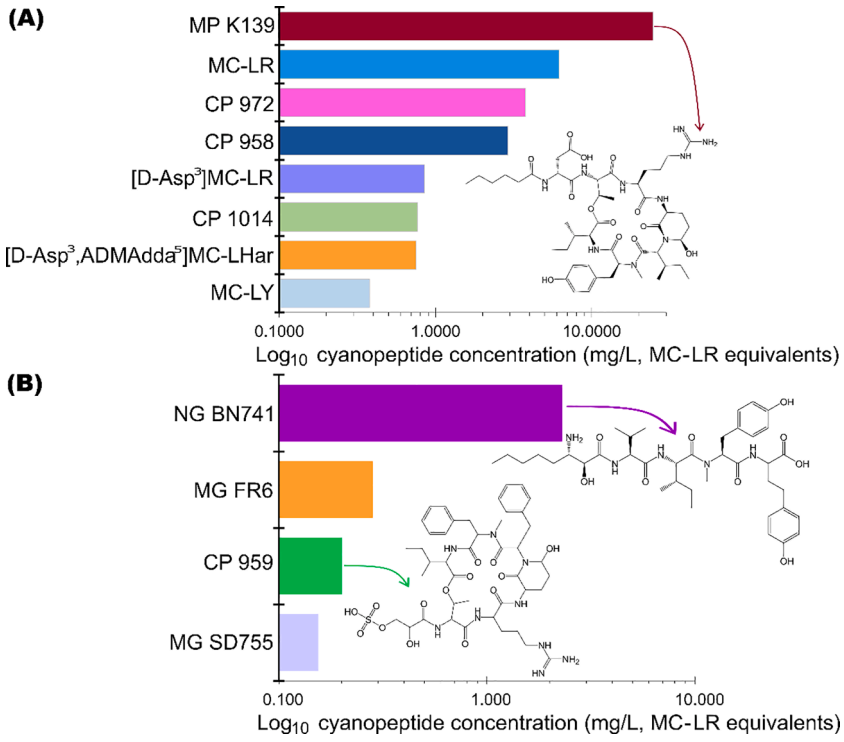

Fig. 1. Concentration of cyanopeptides produced by (A) *Microcystis panniformis* MIRS-04 and (B) *Microcystis aeruginosa* NPCD-01, expressed as mg/L of MC-LR equivalents (i.e. based on using MC-LR external calibration curve for quantification). Values reflect the highest exposure concentration employed in the toxicity tests of the pooled extract for micropeptins (MP), microcystins (MC), cyanopeptolins (CP), nostoginin (NG) and microginins (MG).

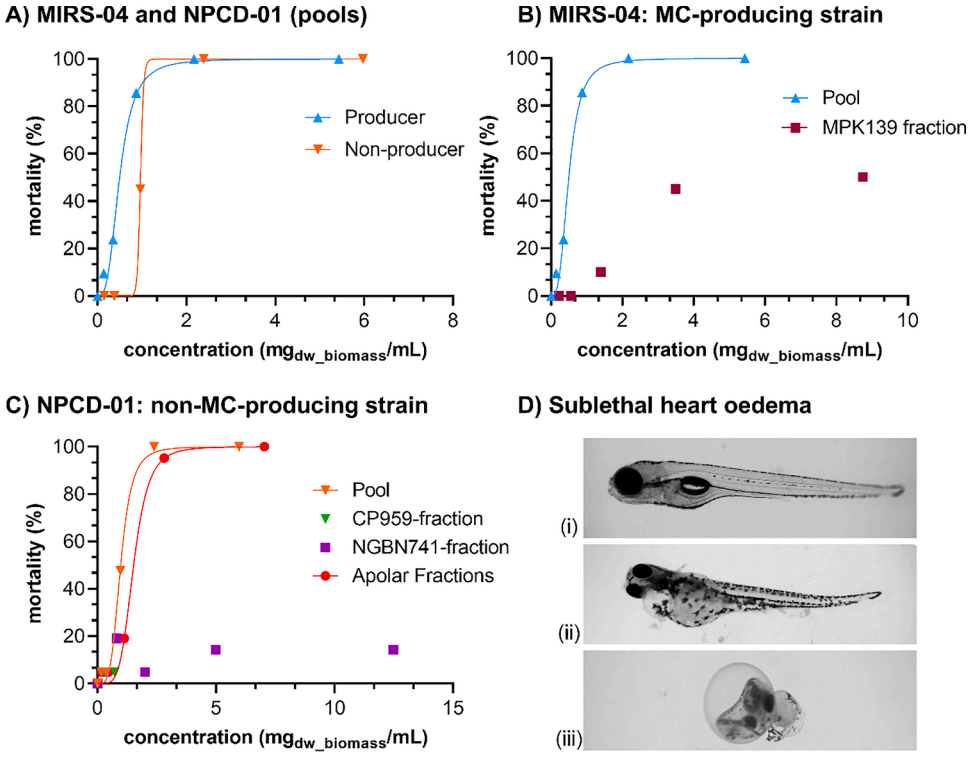

Fig. 2. Dose-response mortality curves of zebrafish larvae relative to mg dry biomass equivalents ($mg_{dw\_biomass}$/mL) at 120 hpf, following exposure to varying concentrations of (A) all pooled HPLC-fractions of MIRS-04 (blue up-triangles) and NPCD-01 (orange down-triangles); (B) a pool of all HPLC fractions from MIRS-04 (blue up-triangles) and the specific HPLC fraction from MIRS-04 containing primarily micropeptin K139 (dark-red squares); (C) a pool of all HPLC fractions from NPCD-01 and the individual HPLC fractions from NPCD-01 containing mainly nostoginin-BN741 (purple squares), cyanopeptolin-959 (green down-triangles) and apolar compounds ('apolar fractions'; red circles); and (D) microscope images (x3 magnification) of a healthy zebrafish larvae from the control wells (i) versus representative examples of larvae with heart oedema following exposure to MIRS-04 fraction #7 (micropeptin K139 at 18.32 mg/L, C1) (ii) and NPCD-01 fraction #3 (nostoginin-BN741 at 2.91 mg/L, C1) (iii).

Figure SI4A+*B*). These observations suggest that micropeptin K139 contributed significantly to the observed toxicity in the pooled extract, and the remaining lethal toxicity may be linked to microcystins and other metabolites present in other fractions. Studies exploring the acute toxicity of microcystins in zebrafish embryos are limited. Wei et al. (2020) reported LC_{50} of 2.79 mg/L for MC-LR (72 hpf zebrafish embryos). The LC_{50} value for MC-LR observed by Wei et al. (2020) is 2.6-fold higher than the concentration in our study at the LC_{50} level (0.7 mg/L MC-LR, other microcystins contributed less than 0.02 mg/L), and further supports that micropeptin K139 contributed significantly to

mortality.

Of the HPLC fractions derived from NPCD-01 - a non-producer of microcystins - the nostoginin BN741-dominated fraction (fraction #3 with RT 8–10 min, 97.2% by peak area, Figure SI1A) and the cyanopeptolin 959-dominated fraction (fraction #1 with RT 4–16 min, 73.3% by peak area, Figure SI1B) were inspected separately. Exposure of *D. rerio* embryos to the nostoginin BN741-dominated fraction resulted in low mortality, with the two highest concentrations (12.48 and 4.99 $mg_{dw\_biomass}$/mL, respectively, Fig. 2C) causing 14% lethality. The cyanopeptolin 959-dominated fraction could only be tested at low concentrations, at which it did not induce acute lethal effects. We conclude that the two most abundant cyanopeptides in NPCD-01 (based on peak area), nostoginin BN741 and cyanopeptolin 959, do not contribute significantly to the mortality induced through exposure of zebrafish embryos to the *pooled fractions* of NPCD-01 (assuming they do not have additive or synergistic modes of actions). Further inspection of the remaining HPLC fractions revealed that the apolar fractions (fraction #9 + 10, RT 20–24 min, eluted at 95% methanol in the HPLC separation) were the main contributors to the acute toxicity, resulting in LC_{50} values at 120 hpf of 1.52 $mg_{dw\_biomass}$/mL (Fig. 2C). Suspect screening of the apolar fractions against CyanoMetDB lead to no conclusive matches of known cyanobacterial metabolites. However, untargeted screening of metabolites using the MolNetEnhancer tool from the Global Natural Products Social Molecular Networking (GNPS) pointed to the presence of glycerolipids, the most abundant one being identified glyceryl palmitate (Figure SI27). It is worth mentioning that the same data analysis pipeline (molecular networking and MolNetEnhancer) was applied to analyse the apolar fractions of the MIRS strain, but the apolar glycerolipids tentatively identified in the NPCD strain were not found, pointing to differences in their respective metabolite profiles.

In a recent study, Roegner et al. (2019) observed high mortality and developmental impairment in zebrafish embryos exposed to lipophilic extracts of *Microcystis* bloom samples from the La Plata river, Uruguay (extract of 1 mg dry with biomass/mL). Similarly, in a toxicity screening study, Berry et al. (2007) tested over 122 cyanobacterial polar (EtOH) and apolar ($CHCl_3$) extracts with the zebrafish developmental toxicity assay. Of those, the majority of the toxic extracts were lipophilic, and all embryos exposed to concentrations of 50 μg/mL or higher were found to die within 24 h, regardless of developmental stage. Fish eggs and embryos can rapidly achieve high tissue concentrations of hydrophobic chemicals present at very low concentrations in the surrounding water (Incardona and Scholz 2016), and the more pronounced effect of lipophilic compounds from cyanobacterial extracts on the embryo development is presumably due to the ability of those compounds to more easily cross the protective chorion and or other membrane barriers of zebrafish embryos (Lydon et al., 2022; Berry et al., 2007; Roegner et al., 2019). The correlation of lipophilicity and hydrophobicity, and the embryo uptake in the zebrafish model was previously documented (Lydon et al., 2022 and references therein). Amongst these studies, different levels of developmental toxicity were observed in embryos, dependant on the lipophilic extract tested (different bloom samples or different cyanobacterial strain biomasses). Such differences suggest that the developmental impairment observed in the fish is related to the presence of specific metabolites in some of the apolar fractions, while for others the toxic effects are rather caused by more general baseline toxicity of the as-yet unidentified apolar compounds, as highlighted by Berry et al. (2007).

We emphasise that the acute toxicity observed in the apolar fractions herein might not only be explained or attributed to the metabolites identified in the untargeted screening in our study, considering that their composition was not exhaustively elucidated, and toxicity was also observed in aqueous extracts by Fernandes et al. (2019). To conclude, the mortality observed for the microcystin-free fraction of MIRS-04 and the extract of NPCD-01, a non-microcystin producer, further adds to the existing body of literature that cyanobacterial metabolites other than microcystins can cause acute (lethal) toxicological effects. We investigated further sublethal toxicity endpoints for those concentrations and fractions where no or low acute effects were observed and where enough individuals survived to facilitate investigation of morphological and behavioural effects.

3.3. Sublethal morphological effects

Type and frequency of sublethal effects and morphological abnormalities were monitored in zebrafish larvae exposed to pooled and individual HPLC fractions, derived from both MIRS-04 and NPCD-01 extracts. The sublethal endpoints included observations of malformation in the 120 hpf larvae, such as oedema of the pericardial region; yolk deformations; malformation of the tail; general delay of development; malformation of the head; modified axis structure; yolk oedema; and no reaction to physical trigger.

Here, both the NPCD-01 *pooled fractions* and the nostoginin BN741-containing fraction (fraction #3), tested separately, showed increased frequency of oedema of the pericardial region at all concentrations tested (Table 2, Fig. 2D). The nostoginin BN741-fraction also prevented hatching in all affected larvae. The cyanopeptolin-959-containing fraction (fraction #1), which showed no lethal effects, also did not trigger sublethal effects in zebrafish embryos. For the microcystin-producing MIRS-04 strain, the *pooled fractions* did not elicit sublethal effects. However, the micropeptin K139-containing fraction (fraction #7) derived from MIRS-04 caused oedema of the pericardial region.

Next, morphological parameters including body length, swim bladder and eye sizes, as well as changes in the heart rate (cardiological effects), were assessed for larvae exposed to the pooled and individual fractions from both cyanobacterial strains. Measurements were performed in all surviving larvae, unless severely deformed. The results were statistically compared to corresponding controls (Kruskal–Wallis one-way analysis of variance, followed by Dunn's test). Heart rates and body length were only affected in larvae exposed to the MIRS-04 *pooled fractions* at 0.35 $mg_{dw\_biomass}$/mL (concentration C4, Fig. 3), which approximately matches the estimated LC_{50} range (0.34–0.52 $mg_{dw\_biomass}$/mL). At this concentration, 16 out of 21 larvae survived, and a higher concentration could not be considered due to high rates of mortality, i.e., two or fewer larvae survived. The micropeptin-K139-containing fraction from MIRS-04, did not significantly affect these other morphological endpoints in larvae that had survived and that were not already affected by oedema of the pericardial region (Figure SI5).

Exposure of zebrafish embryos to the NPCD-01 *pooled fractions* at 0.96 $mg_{dw\_biomass}$/mL, around the LC_{50} range (0.89–1.07 $mg_{dw\_biomass}$/mL), appeared to lower heart rates versus solvent control, though results were not statistically significant ($p<0.1$, concentration C3 in Figure SI6). The apolar fraction from NPCD-01 showed similar LC_{50} values as the pooled fractions and also showed a trend of lower heart rates exposed at 1.13 $mg_{dw\_biomass}$/mL, differing significantly from the controls ($p<0.05$), despite the pericardial area showing no significant variations (concentration C3 in Figure SI7). Heart rate and morphological measurements of larvae were not significantly affected when exposed to any concentration of the cyanopeptolin-959-containing fraction (fraction #1) nor the nostoginin BN741-containing fraction (fraction #3) from NPCD-01 ($p>0.05$, Figures SI8–9).

Roegner et al. (2019) exposed zebrafish embryos to different cyanobacterial metabolites (including known cyanotoxins), and reported that, of the 24 different metabolites tested, only cylindrospermopsin, [D-Asp^3]-MC-RR, L-BMAA, lyngbyatoxin-a, MC-LR and MC-RR resulted in significant embryo mortality at 120 hpf. However, similar to our findings, the authors observed pericardial or yolk sac oedema in embryos exposed to microcystins MC-LA and MC-HilR, and to non-microcystin cyanobacterial metabolites, including: cyanopeptolin 1040, microginin 690, anabaenopeptin B and anatoxin-a. Recently, Jacinavicius et al. (2023) observed oedema in the pericardial and digestive system regions of zebrafish larvae exposed to different cyanobacterial total extracts (including aquatic and terrestrial strains). The

Table 2

Microcystis aeruginosa (NPCD-01, non-producer)										
Pooled fractions										
Exposure group	Total exposed larvae (alive)	Total affected larvae	Frequency and types of morphological alterations observed							
			OPC	YD	MT	D	MH	A	YE	NR
5.97 mg/mL	0	0	-	-	-	-	-	-	-	-
2.39 mg/mL	0	0	-	-	-	-	-	-	-	-
0.96 mg/mL	12	1	1/1	0	1/1	1/1	1/1	0	1/1	0
0.38 mg/mL	21	2	2/1	1/2	0	0	1/2	0	1/2	0
0.15 mg/mL	22	3	3/3	1/3	1/3	1/3	1/3	0	1/3	1/3
SC	33	1	1/1	0	0	0	0	0	0	0
NC	31	2	1/2	1/2	0	0	0	0	0	0
Cyanopeptolin 959-containing fraction (#1)										
Exposure group	Total exposed larvae (alive)	Total affected larvae	Frequency and types of morphological alterations observed							
			OPC	YD	MT	D	MH	A	YE	NR
11.27 mg/mL	21	0	0	0	0	0	0	0	0	0
4.51 mg/mL	21	0	0	0	0	0	0	0	0	0
1.80 mg/mL	21	0	0	0	0	0	0	0	0	0
0.72 mg/mL	21	1	1/1	0	0	0	0	0	0	0
0.29 mg/mL	20	0	0	0	0	0	0	0	0	0
SC	37	1	1/1	0	0	0	0	0	0	0
NC	34	0	0	0	0	0	0	0	0	0
Nostoginin BN741-containing fraction (#3)										
Exposure group	Total exposed larvae (alive)	Total affected larvae	Frequency and types of morphological alterations observed							
			OPC	YD	MT	D	MH	A	YE	NR
12.48 mg/mL	21	3	2/3	0	0	1/3	1/3	0	1/3	0
4.99 mg/mL	21	3	3/3	0	0	0	0	0	0	0
1.99 mg/mL	21	1	1/1	0	0	0	0	0	0	0
0.80 mg/mL	21	4	4/4	1/4	0	1/4	0	0	0	0
0.32 mg/mL	21	1	0	0	0	1/1	0	0	0	0
SC	37	0	0	0	0	0	0	0	0	0
NC	34	1	0	0	0	1/1	0	0	0	0
Apolar fractions (#9+10)										
Exposure group	Total exposed larvae (alive)	Total affected larvae	Frequency and types of morphological alterations observed							
			OPC	YD	MT	D	MH	A	YE	NR
7.04 mg/mL	0	0	0	0	0	0	0	0	0	0
2.81 mg/mL	1	0	0	0	0	0	0	0	0	0
1.13 mg/mL	17	2	2/2	0	0	1/2	2/2	0	0	0
0.45 mg/mL	20	0	0	0	0	0	0	0	0	0
0.18 mg/mL	20	0	0	0	0	0	0	0	0	0
SC	35	1	0	0	0	0	0	1/1	0	0
NC	32	1	1	0	1/1	1/1	1/1	0	1/1	0
Microcystis panniformis (MIRS-04, MC-producer)										
Pooled fractions										
Exposure group	Total exposed larvae (alive)	Total affected larvae	Frequency and types of morphological alterations observed							
			OPC	YD	MT	D	MH	A	YE	NR
5.43 mg/mL	0	0	-	-	-	-	-	-	-	-
2.17 mg/mL	0	0	-	-	-	-	-	-	-	-
0.87 mg/mL	2	1	1/1	0	0	0	0	0	0	0
0.35 mg/mL	16	0	0	0	0	0	0	0	0	0
0.14 mg/mL	19	0	0	0	0	0	0	0	0	0
SC	32	5	5/5	1/5	0	4/5	1/5	0	0	0
NC	30	4	3/4	1/4	1/4	3/4	1/4	0	0	0
Micropeptin K139-containing fraction (#7)										
Exposure group	Total exposed larvae (alive)	Total affected larvae	Frequency and types of morphological alterations observed							
			OPC	YD	MT	D	MH	A	YE	NR
8.74 mg/mL	10	4	3/4	2/4	0	0	0	0	0	3/4
3.49 mg/mL	11	2	1/2	0	2/2	0	0	1/2	0	1/2
1.40 mg/mL	18	2	2/2	0	0	0	0	0	1/2	0
0.56 mg/mL	20	1	1/1	1/1	0	0	0	0	1/1	0
0.22 mg/mL	20	1	1/1	0	0	0	0	0	1/1	0
SC	37	0	0	0	0	0	0	0	0	0
NC	34	0	0	0	0	0	0	0	0	0

OPC: oedema of the pericardial region; YD: yolk deformations; MT: malformation of the tail; D: general delay of development; MH: malformation of the head; A: modified axis structure; YE: yolk oedema; NR: no reaction to trigger; SC: solvent control; NC: negative control. Concentrations refer to mg of dry weight of biomass equivalents per mL.

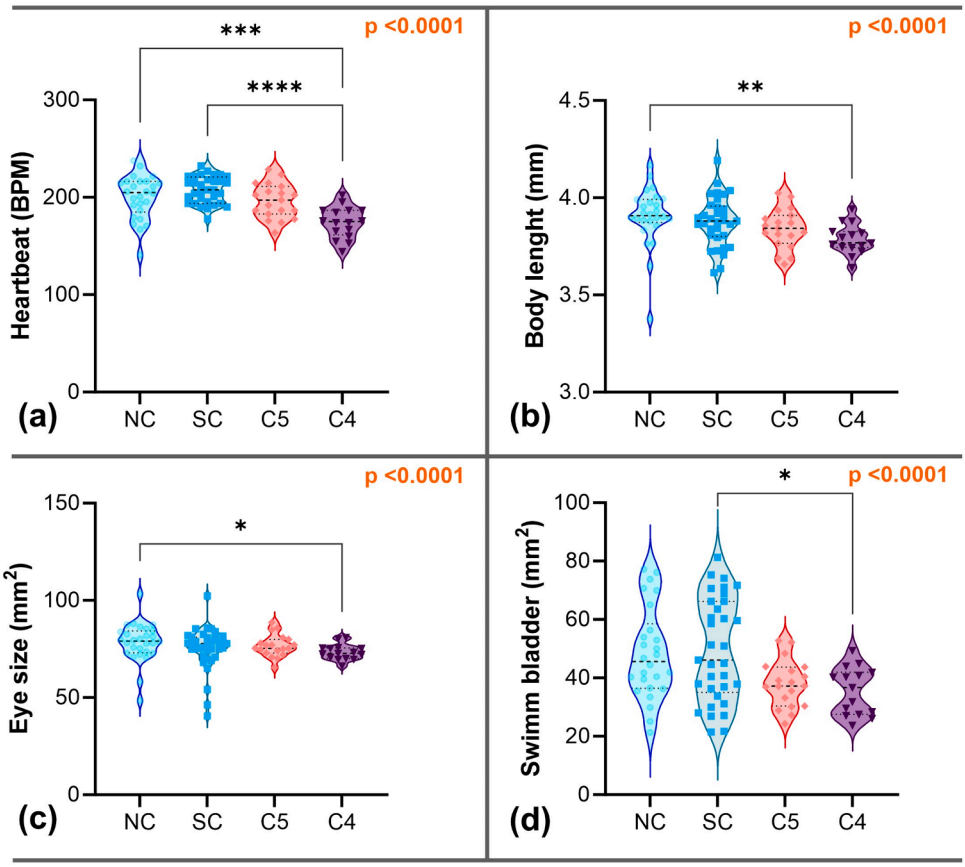

Fig. 3. Heartbeat(a), body length (b), eye size (c), and swim bladder size (d) measured of surviving larvae exposed to MIRS-04 pooled fractions (120 hpf) at the second to lowest and lowest concentration levels tested (C4 = 0.35 mg_{dw}/mL and C5 = 0.14 mg_{dw}/mL, respectively) and for the negative control (NC) and the solvent control (SC). The p values reported refer to the Kruskal–Wallis one-way ANOVA. Significant alterations between groups in the post-hoc Dunn's for multiple comparisons are indicated by asterisks (*$p < 0.05$; **$p < 0.01$; ***$p < 0.001$; ****$p < 0.0001$).

authors highlighted the rich structural diversity of peptides and lipopeptides produced by the toxic strains.

Overall, morphological assessments suggest that micropeptin K139 can contribute to lethal toxicity and oedema of the pericardial region; nostoginin BN741 also contributes to oedema of the pericardial region and affects hatching but does not contribute to acute mortality at the concentrations tested. As mentioned previously, many cyanopeptolin and microginin variants showed inhibitory activity against different serine proteases. Micropeptin K139 was proven to be a potent FVIIa-sTF inhibitor (EC_{50} = 10.62 μM), and a thrombin inhibitor (EC_{50} = 26.94 μM) (Anas et al., 2017). In zebrafish, Protease Activated Receptors (PARs) were shown to regulate the development and differentiation of the lymphatic system (Lei et al., 2021), and amongst the PAR upstream proteases, thrombin, plasmin, factor Xa, factor VIIa, trypsin, and matrix metalloproteases have been identified. We hypothesise that the cardiovascular effects observed in zebrafish (i.e., oedema of the pericardial region), may arise through inhibition of the proteases, though further studies exploring in vivo inhibition of proteases would be required to test this hypothesis.

Lastly, the disruption of cardiac function during early organogenesis in fish larvae can subsequently alter cardiac morphology and function, initiating a cascade of adverse effects on cardiorespiratory and physiological performance (Incardona and Scholz 2016). The extent of the observed cardiological sublethal effects suggests that exposure to these concentrations of nostoginin BN741 and micropeptin K139 can potentially compromise the development and physiological performance of the fish and, as a consequence, its survival.

3.4. Behavioural effects

The behaviour tracking assay consisted of different phases: acclimation phase (20 min in light) (I); spontaneous swimming behaviour in light (20 min) (II); two alternated dark intervals of 10 min ("dark intervals", lII and V); and two alternated light intervals of 10 min ("light intervals", IV and VI). The light-dark transition test in early life stages of zebrafish is frequently used to assess developmental neurotoxicity (Könemann et al., 2022), and each phase is illustrated in Fig. 4. The peaks of increased locomotor activity normally occurring in unexposed zebrafish larvae can be noted in the dark intervals (III and V), known as light seeking behaviour.

In addition to the acute and sublethal effects observed, exposure of zebrafish larvae to MIRS-04 *pooled fractions* at 0.35 $mg_{dw\_biomass}$/mL (C4) caused a significant decrease in locomotor activity during the dark stages, compared to observations in larvae exposed at 0.14 mg_{dw}/mL (C5) and to controls ($p<0.05$, Fig. 4). At 0.35 $mg_{dw\_biomass}$/mL, approximately 0.5 mg/L of total MCs identified (Table 1) were present in the *pooled fractions* along with the other co-produced metabolites listed. No significant changes in locomotor behaviour were observed for larvae exposed to micropeptin-containing fraction #7 (MIRS-04), NPCD-01's *pooled fractions*, or nostoginin-containing fraction #3 from NPCD-01 (Figures SI10–14). Note, that in some cases, the locomotor activity of exposed larvae differed significantly from the negative control in the dark phase but not from the solvent control. The solvent control, in turn, was then not significantly different from negative control (Figures SI10–14).

Few recent studies suggest that the adverse effects on zebrafish

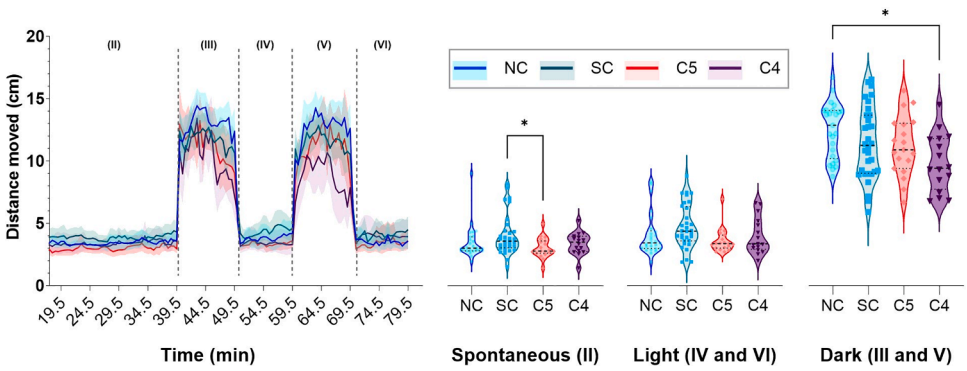

Fig. 4. Time series of the accumulated distance moved, recorded every 30 s, and boxplots representing the average distance moved in each phase of the behaviour assay - spontaneous, light intervals, and dark intervals - of larvae exposed to different concentrations of MIRS-04 pooled fractions. On boxplots, alterations between groups obtained by Kruskal–Wallis one-way analysis of variance, followed by Dunn's multiple comparison test (95% confidence interval) are indicated by asterisks (*$p < 0.05$). NC: Negative control; SC: Solvent control, C4: 0.35 mg_{dw}/mL; C5: 0.14 mg_{dw}/mL.

locomotor activity caused by microcystins, may be enhanced during co-exposure with other toxins and metabolites (Martin et al., 2021; Qian et al., 2018; Yu et al., 2021). Martin et al. (2021) assessed the effect of MC-LR exposure and observed no effect on general locomotive activity up to 1 mg/L. By contrast, Qian et al. (2018) observed decreased general locomotor activity upon exposure to *Microcystis* aeruginosa extract that contained considerably lower concentrations of MC-LR (0.275–0.592 mg/L), along with co-produced metabolites that were not further determined. Martin et al. (2012) also observed increased acoustic startle sensitivity at 1 mg/L MC-LR, which was reduced to 0.1 mg/L when co-exposed with another toxins (BMAA at 100 μM). Herein, we observed reduced locomotive activity upon exposure to the *pooled fractions* of the MC producer (MIRS-04) at similar MCs concentrations (0.7 mg/L) as Qian et al. (2018).

4. Conclusion

Our results further add to the existing body of literature highlighting that cyanobacterial metabolites other than microcystins can cause acute lethal and sublethal toxicological effects in fish larvae. We have confirmed that the NPCD-01 strain does not synthesise microcystins, yet inflicts comparable lethality in zebrafish larvae to that induced by the microcystin-producing MIRS-04 strain. Our results suggest that the toxicity of the non-producer NPCD-01 was mostly prompted by lipophilic compounds present in the apolar fractions of the extract. We demonstrated that micropeptin K139, a cyanopeptolin, can significantly contribute to lethal toxicity and cause oedema of the pericardial region. We further revealed that nostoginin BN741, a microginin, also contributes to oedema of the pericardial region and impedes hatching, without inducing lethal effects. Based on previous studies of cyanopeptolins and microginins, we hypothesise that the cardiovascular effects observed in zebrafish upon exposure to micropeptin K139 and nostoginin BN741, may be linked to protease inhibition. Our observations further support the sparse body of literature on mixture toxicity of microcystins and other metabolites towards the neurotoxicological potential on the nervous system of zebrafish.

Our results highlight the need for further investigations into the specific hazards posed by diverse cyanobacterial metabolites beyond those currently considered under WHO water quality guidelines. This is especially crucial given the increased frequency with which bloom events are now occurring across the globe, particularly in tropic, developing countries. Our results strengthen the foundation for a better mechanistic understanding of toxicity and mode of action of protease inhibiting cyanopeptides, which is important for predicting adverse outcomes in fish and other organisms, including humans. The evidence of diverse sublethal effects of other metabolites and the fact that cyanobacteria always co-produce a range of secondary metabolites, emphasize the need to assess risk in light of mixture toxicities rather than individual toxins only. Overall, our study contributes to a better understanding of the hazards caused by specific cyanopeptides and helps guide the regulation and management of cyanotoxins in the aquatic environments.

Authors' contributions

MAT: conceptualization, investigation, experimental analysis, data evaluation and visualization, writing (original draft), and editing. MJ: experimental analysis, data evaluation, reviewing, and editing writing (final draft). CvB: conceptualization, data evaluation, reviewing, and editing writing; EP: conceptualization, data evaluation, reviewing, and editing writing; EJ: supervision, conceptualization, data evaluation, reviewing, and editing writing. All authors read and approved the final manuscript.

Declaration of Competing Interest

The authors declare the following financial interests/personal relationships which may be considered as potential competing interests:

Mariana de Almeida Torres reports a relationship with Eawag Swiss Federal Institute of Aquatic Science and Technology that includes: funding grants. Mariana de Almeida Torres reports a relationship with Coordination for the Improvement of Higher Education Personnel that includes: funding grants. Ernani Pinto reports a relationship with São Paulo State Research Foundation that includes: funding grants. Ernani Pinto reports a relationship with University of São Paulo Foundation that includes: funding grants.

Data availability

Data will be made available on request.

Acknowledgements

The authors thank Dr Christopher O. Miles for the help with identifying cyanobacterial metabolites. MAT acknowledges Coordination for the Improvement of Higher Education Personnel – CAPES (grant 88882.327686/2019–01) for the PhD scholarship, and Eawag for the Partnership Programme for Developing Countries; EP acknowledges São Paulo State Research Foundation – FAPESP (grant 2021/00149–0), University of São Paulo Foundation – FUSP (project #1979), and the Brazilian National Council for Scientific and Technological Development – CNPq (grant 439065/2018–6). Graphical abstract was created with BioRender.

Supplementary materials

Supplementary material associated with this article can be found, in the online version, at doi:10.1016/j.aquatox.2023.106689.

References

Anas, A.R.J., Mori, A., Tone, M., Naruse, C., Nakajima, A., Asukabe, H., Takaya, Y., Imanishi, S.Y., Nishizawa, T., Shirai, M., Harada, K.I., 2017. FVIIa-sTF and thrombin inhibitory activities of compounds isolated from *Microcystis aeruginosa* K-139. Mar. Drugs 15, 1–13. https://doi.org/10.3390/md15090275.

Azevedo, S.M.F.O., Carmichael, W.W., Jochimsen, E.M., Rinehart, K.L., Lau, S., Shaw, G. R., Eaglesham, G.K., 2002. Human intoxication by microcystins during renal dialysis treatment in Caruaru - Brazil. Toxicology 181–182, 441–446. https://doi.org/10.1016/S0300-483X(02)00491-2.

Bambino, K., Chu, J., 2017. Zebrafish in toxicology and environmental health. Current Topics in Developmental Biology, 1st ed. Elsevier Inc. https://doi.org/10.1016/bs.ctdb.2016.10.007.

Berry, J.P., Gantar, M., Gibbs, P.D.L., Schmale, M.C., 2007. The zebrafish (*Danio rerio*) embryo as a model system for identification and characterization of developmental toxins from marine and freshwater microalgae. Comp. Biochem. Physiol. - C Toxicol. Pharmacol. 145, 61–72. https://doi.org/10.1016/j.cbpc.2006.07.011.

Blagojević, D., Babić, O., Kaišarević, S., Stanić, B., Mihajlović, V., Davidović, P., Marić, P., Smital, T., Simeunović, J., 2021. Evaluation of cyanobacterial toxicity using different biotests and protein phosphatase inhibition assay. Environ. Sci. Pollut. Res. 28, 49220–49231. https://doi.org/10.1007/s11356-021-14110-2.

Chorus, I., Bartram, J., 1999. Toxic Cyanobacteria in Water : A guide to Their Public Health consequences, Monitoring and Management. E & FN Spon, on behalf of the World Health Organisation, London, UK.

Chorus, I., Welker, M., 2021. Toxic Cyanobacteria in Water - A Guide to Their Public Health Consequences, Monitoring and Management, 2nd Edition. CRC Press, Boca Raton (FL), on behalf of the World Health Organization (WHO), Geneva, CH.

Di Paolo, C., Groh, K.J., Zennegg, M., Vermeirssen, E.L.M., Murk, A.J., Eggen, R.I.L., Hollert, H., Werner, I., Schirmer, K., 2015. Early life exposure to PCB126 results in delayed mortality and growth impairment in the zebrafish larvae. Aquat. Toxicol. 169, 168–178. https://doi.org/10.1016/j.aquatox.2015.10.014.

do Nascimento, E.L., Koschek, P.R., dos Santos, M.E.V., Pacheco, A.B.F., Gomes, A.M., da, A., de Souza, C.M.M., Bastos, W.R., de Oliveira Azevedo, S.M.F., 2021. Influence of iron on physiological parameters and intracellular microcystin in *Microcystis Panniformis* strain isolated from a reservoir in the amazon. Curr. Microbiol. 78, 2345–2354. https://doi.org/10.1007/s00284-021-02499-5.

Ernst, M., Kang, K.Bin, Caraballo-Rodríguez, A.M., Nothias, L.F., Wandy, J., Chen, C., Wang, M., Rogers, S., Medema, M.H., Dorrestein, P.C., van der Hooft, J.J.J., 2019. Molnetenhancer: enhanced molecular networks by integrating metabolome mining and annotation tools. Metabolites 9. https://doi.org/10.3390/metabo9070144.

Fernandes, K., Gomes, A., Calado, L., Yasui, G., Assis, D., Henry, T., Fonseca, A., Pinto, E., 2019. Toxicity of cyanopeptides from two microcystis strains on larval development of *Astyanax altiparanae*. Toxins (Basel) 11, 2–6. https://doi.org/10.3390/toxins11040220.

Filatova, D., Jones, M.R., Haley, J.A., Núñez, O., Farré, M., Janssen, E.M.L., 2021. Cyanobacteria and their secondary metabolites in three freshwater reservoirs in the United Kingdom. Environ. Sci. Eur. 33 https://doi.org/10.1186/s12302-021-00472-4.

Fitzgerald, J.A., Kirla, K.T., Zinner, C.P., vom Berg, C.M., 2019. Emergence of consistent intra-individual locomotor patterns during zebrafish development. Sci. Rep. 9, 1–14. https://doi.org/10.1038/s41598-019-49614-y.

Gorham, P.R., McLachlan, J., Hammer, U.T., Kim, W.K., 1964. Isolation and culture of toxic strains of *Anabaena flos-aquae* (Lyngb.) de Bréb. In: SIL Proceedings, 1922-2010 15, pp. 796–804. https://doi.org/10.1080/03680770.1962.11895606.

Huang, I.S., Zimba, P.V., 2019. Cyanobacterial bioactive metabolites—a review of their chemistry and biology. Harmful Algae 83, 42–94. https://doi.org/10.1016/j.hal.2018.11.008.

Huisman, J., Codd, G.A., Paerl, H.W., Ibelings, B.W., Verspagen, J.M.H., Visser, P.M., 2018. Cyanobacterial blooms. Nat. Rev. Microbiol. 16, 471–483. https://doi.org/10.1038/s41579-018-0040-1.

Incardona, J.P., Scholz, N.L., 2016. The influence of heart developmental anatomy on cardiotoxicity-based adverse outcome pathways in fish. Aquat. Toxicol. 177, 515–525. https://doi.org/10.1016/j.aquatox.2016.06.016.

Ishida, K., Kato, T., Murakami, M., Watanabe, M., Watanabe, M.F., 2000. Microginins, zinc metalloproteases inhibitors cyanobacterium *Microcystis aeruginosa*. Tetrahedron 56, 8643–8656. https://doi.org/10.1016/S0040-4020(00)00770-5.

ISO, 1996. ISO 7346-3:1996 - water quality — determination of the acute lethal toxicity of substances to a freshwater fish [*Brachydanio rerio* Hamilton-Buchanan (Teleostei, Cyprinidae)] — Part 3: flow-through method. International Standards.

Jacinavicius, F.R., Geraldes, V., Fernandes, K., Crnkovic, C.M., Gama, W.A., Pinto, E., 2023. Toxicological effects of cyanobacterial metabolites on zebrafish larval development. Harmful Algae 125, 102430. https://doi.org/10.1016/j.hal.2023.102430.

Janssen, E.M.L., 2019. Cyanobacterial peptides beyond microcystins – a review on co-occurrence, toxicity, and challenges for risk assessment. Water Res 151, 488–499. https://doi.org/10.1016/j.watres.2018.12.048.

Janssen, E.M.-L., Jones, M.R., Pinto, E., Dörr, F., Torres, M.A, Rios Jacinavicius, F., Mazur-Marzec, H., Szubert, K., Konkel, R., Tartaglione, L., Dell'Aversano, C., Miglione, A., McCarron, P., Beach, D.G., Miles, Ch.O., Fewer, D.P., Sivonen, K., Jokela, J., Wahlsten, M., Niedermeyer, T.H.J., Schanbacher, F., Leão, P., Preto, M., D'Agostino, P.M., Baunach, M., Dittmann, E., Reher, R., Schymanski, E. Dataset S75, CyanoMetDB - Comprehensive database of secondary metabolites from cyanobacteria. Zenodo, 2023, https://zenodo.org/record/4551528.

Jones, M.R., Pinto, E., Torres, M.A., Dörr, F., Mazur-Marzec, H., Szubert, K., Tartaglione, L., Dell'Aversano, C., Miles, C.O., Beach, D.G., McCarron, P., Sivonen, K., Fewer, D.P., Jokela, J., Janssen, E.M.L., 2021. CyanoMetDB, a comprehensive public database of secondary metabolites from cyanobacteria. Water Res 196, 117017. https://doi.org/10.1016/j.watres.2021.117017.

Kimmel, C.B., Ballard, W.W., Kimmel, S.R., Ullmann, B., Schilling, T.F., 1995. Stages of embryonic development of the zebrafish. Dev. Dyn. 203, 253–310. https://doi.org/10.1002/aja.1002030302.

Köcher, S., Resch, S., Kessenbrock, T., Schrapp, L., Ehrmann, M., Kaiser, M., 2020. From dolastatin 13 to cyanopeptolins, micropeptins, and lyngbyastatins: the chemical biology of Ahp-cyclodepsipeptides. Nat. Prod. Rep. 37, 163–174. https://doi.org/10.1039/c9np00033j.

Könemann, S., Von Wyl, M., Vom Berg, C., 2022. Zebrafish larvae rapidly recover from locomotor effects and neuromuscular alterations induced by cholinergic insecticides. Environ. Sci. Technol. 56, 8449–8462. https://doi.org/10.1021/acs.est.2c00161.

Lei, D., Zhang, Xiuru, Rouf, M.A., Mahendra, Y., Wen, L., Li, Y., Zhang, Xiaojuan, Li, L., Wang, L., Zhang, T., Wang, G., Wang, Y., 2021. Noncanonical protease-activated receptor 1 regulates lymphatic differentiation in zebrafish. iScience 24. doi:10.1016/j.isci.2021.103386.

Lodin-Friedman, A., Carmeli, S., 2018. Microginins from a *Microcystis sp*. Bloom material collected from the kishon reservoir, Israel. Mar. Drugs 16. https://doi.org/10.3390/md16030078.

Lydon, C.A., Mejia-fava, J., Collado-vides, L., Eskelinen, H., Berry, J.P., 2022. Identification of apparently neurotoxic metabolites from assemblages of marine filamentous cyanobacteria associated with the intoxication of captive bottlenose dolphins (*Tursiops truncatus*) in the Florida Keys. Chemosphere 288, 132423. https://doi.org/10.1016/j.chemosphere.2021.132423.

Malbrouck, C., Kestemont, P., 2006. Effects of microcystins on fish. Environ. Toxicol. Chem. 25, 72–86. https://doi.org/10.1897/05-029R.1.

Martin, R.M., Bereman, M.S., Marsden, K.C., 2021. BMAA and MCLR interact to modulate behavior and exacerbate molecular changes related to neurodegeneration in larval zebrafish. Toxicol. Sci. 179, 251–261. https://doi.org/10.1093/toxsci/kfaa178.

Mazur-Marzec, H., Fidor, A., Cegłowska, M., Wieczerzak, E., Kropidłowska, M., Goua, M., Macaskill, J., Edwards, C., 2018. Cyanopeptolins with trypsin and chymotrypsin inhibitory activity from the cyanobacterium *Nostoc edaphicum* CCNP1411. Mar. Drugs 16, 1–19. https://doi.org/10.3390/md16070220.

Merel, S., Walker, D., Chicana, R., Snyder, S., Baurès, E., Thomas, O., 2013. State of knowledge and concerns on cyanobacterial blooms and cyanotoxins. Environ. Int. 59, 303–327. https://doi.org/10.1016/j.envint.2013.06.013.

Nagarajan, M., Maruthanayagam, V., Sundararaman, M., 2013. SAR analysis and bioactive potentials of freshwater and terrestrial cyanobacterial compounds: a review. J. Appl. Toxicol. 33, 313–349. https://doi.org/10.1002/jat.2833.

Natumi, R., Dieziger, C., Janssen, E.M.L., 2021a. Cyanobacterial toxins and cyanopeptide transformation kinetics by singlet oxygen and pH-dependence in sunlit surface waters. Environ. Sci. Technol. 55, 15196–15205. https://doi.org/10.1021/acs.est.1c04194.

Natumi, R., Janssen, E.M.L., 2020. Cyanopeptide co-production dynamics beyond microcystins and effects of growth stages and nutrient availability. Environ. Sci. Technol. 54, 6063–6072. https://doi.org/10.1021/acs.est.9b07334.

Natumi, R., Marcotullio, S., Janssen, E.M.L., 2021b. Phototransformation kinetics of cyanobacterial toxins and secondary metabolites in surface waters. Environ. Sci. Eur. 33 https://doi.org/10.1186/s12302-021-00465-3.

OECD, 2013. Test No. 236: Fish Embryo Acute Toxicity (FET) Test, pp. 1–18.

Paiva, F.C.R., Ferreira, G.M., Trossini, G.H.G., Pinto, E., 2017. Identification, in vitro testing and molecular docking studies of microginins' mechanism of angiotensin-converting enzyme inhibition. Molecules 22, 1–10. https://doi.org/10.3390/molecules22121884.

Pipal, M., Priebojova, J., Koci, T., Blahova, L., Smutna, M., Hilscherova, K., 2020. Field cyanobacterial blooms producing retinoid compounds cause teratogenicity in zebrafish embryos. Chemosphere 241. https://doi.org/10.1016/j.chemosphere.2019.125061.

Qian, H., Liu, G., Lu, T., Sun, L., 2018. Developmental neurotoxicity of *Microcystis aeruginosa* in the early life stages of zebrafish. Ecotoxicol. Environ. Saf. 151, 35–41. https://doi.org/10.1016/j.ecoenv.2017.12.059.

Roegner, A., Truong, L., Weirich, C., Pírez-Schirmer, M., Brena, B., Miller, T.R., Tanguay, R., 2019. Combined *Danio rerio* embryo morbidity, mortality and photomotor response assay: a tool for developmental risk assessment from chronic cyanoHAB exposure. Sci. Total Environ. 697, 134210 https://doi.org/10.1016/j.scitotenv.2019.134210.

Ruttkies, C., Schymanski, E.L., Wolf, S., Hollender, J., Neumann, S., 2016. MetFrag relaunched: incorporating strategies beyond *in silico* fragmentation. J. Cheminform. 8, 1–16. https://doi.org/10.1186/s13321-016-0115-9.

Schymanski, E.L., Jeon, J., Gulde, R., Fenner, K., Ruff, M., Singer, H.P., Hollender, J., 2014. Identifying small molecules via high resolution mass spectrometry: communicating confidence. Environ. Sci. Technol. 48, 2097–2098. https://doi.org/10.1021/es5002105.

Wei, H., Wang, S., Xu, E.G., Liu, J., Li, X., Wang, Z., 2020. Synergistic toxicity of microcystin-LR and Cu to zebrafish (*Danio rerio*). Sci. Total Environ. 713 https://doi.org/10.1016/j.scitotenv.2019.136393.

Whitton, B.A., 2017. Ecology of cyanobacteria II - their diversity in space and time. Handbook of Cyanobacterial Monitoring and Cyanotoxin Analysis. https://doi.org/10.1002/9781119068761.ch2.

Yu, Y., Zhang, Q., Liu, G., Deng, Y., Kang, J., Zhang, F., Lu, T., Sun, L., Qian, H., 2021. Proteomic analysis of zebrafish brain damage induced by *Microcystis aeruginosa* bloom. Sci. Total Environ. 795, 148865 https://doi.org/10.1016/j.scitotenv.2021.148865.